Transactions of the 15th International Conference on
Structural Mechanics in Reactor Technology (SMiRT-15)
Seoul, Korea, August 15-20, 1999

Development of Simplified Reactor Internal Pump System

Shinichi Kawamura[1)], Yuichi Okamura[1)], Hidetoshi Takehara[2)] and Takahisa Kondoh[3)]

1) Tokyo Electric Power Company, Japan
2) Hitachi Works, Hitachi, Ltd., Japan
3) Isogo Nuclear Engineering Center, Toshiba Corporation

ABSTRACT

Reactor Internal Pump (RIP) was adopted for the Reactor Recirculation System of ABWR in place of the conventional external loop system. Ten RIPs replace large external loop pumps and piping, and this contributes significantly to the simplicity attained in ABWR. Further simplicity is sought for the next ABWR by eliminating Motor-Generator (M-G) sets in the power supply system of the RIPs. For this purpose, the moment of inertia of the RIP is increased to achieve appropriate coast down characteristics without the M-G set. The new inertia-increased RIP accommodates a flywheel in its 500mm-longer casing supported by a thicker sleeve nozzle of the Reactor Pressure Vessel (RPV). Design of the RIP, structural feasibility of the new nozzle, and the effects of its increased size on the pump discharge flow are discussed in this study.

1. INTRODUCTION

Reactor Internal Pump (RIP) circulates the reactor coolant in the Reactor Pressure Vessel (RPV) of ABWR. The RIP is a single-stage, mixed-flow pump, which is supported by a nozzle located on the periphery of the RPV bottom head. Ten (10) RIPs replace 20 jet pumps and two external recirculation loops of the Reactor Recirculation System of conventional BWRs. This contributes significantly to the simplicity attained in ABWR, with having advantages of good maintainability, reduction in the occupational radiation exposure, and cost effectiveness.

Further simplicity is sought for the next ABWR by eliminating Motor-Generator (M-G) sets in the power supply system of the RIPs. Because the current RIP has relatively small moment of inertia, a loss of electrical power would cause rapid decrease in the core cooling flow. In order to secure appropriate cooling capacity, two M-G sets are installed for having six RIPs continue to run for a few seconds without external power supply. The elimination of the M-G sets can be achieved by increasing the moment of inertia of the RIP from 19.5 $kg{\cdot}m^2$ to 45 $kg{\cdot}m^2$ [1]. Simplified design of the RIP system with no need for the M-G set is expected to have advantages of improved reliability, less maintenance requirements, and cost reductions.

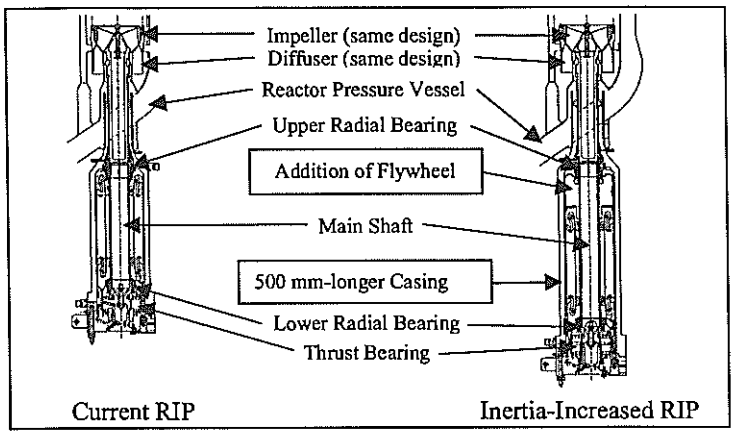

Fig.1 The design of Inertia-Increased RIP.

2. INERTIA-INCREASED RIP

2.1 Design of Inertia-Increased RIP

Fig. 1 shows a comparison between the current RIP and the inertia-increased RIP. The new RIP accommodates a flywheel in its 500 mm-longer casing. However, most of the designs remain unchanged so that the designing, manufacturing and operating experience of the current RIP can be used for the new RIP. The Impeller and the Diffuser are the same as those of the current RIP.

2.2 Critical Speed of the RIP

The bearing span is increased in order to accommodate the flywheel, and its effect on the critical speed of the RIP has been evaluated. The critical speed has been calculated using a simple beam model, and its result shows negligible small difference between the new RIP and the current one. The calculated critical speed of the new RIP is only slightly smaller than the current RIP by about 3%.

2.3 Radial Bearing Load

Radial Bearing load is also affected by the increased bearing span and the weight of the flywheel. Two Radial Bearings support the main shaft against the radial thrust load caused by the fluid force acted on the Impeller and the load caused by the unbalance of the rotating parts. The radial thrust loads can be roughly given by calculating the balance of moments (Eq.1 and Eq.2), and the unbalance load is given by Eq.3;

$$Ra = (L1 + L2) / L2 * F , \quad (1)$$

$$Rb = (L1 / L2) * F , \quad (2)$$

$$Fr = W / g * ((1 + \alpha) * \varepsilon) * (2\pi N / 60)^2 , \quad (3)$$

where Ra and Rb are radial thrust loads on upper and lower Radial Bearings, L1 is distance between the center of gravity of the Impeller and the upper Radial Bearing, L2 is the bearing span, F is fluid force acted on the Impeller, W is the weight of the rotating parts, g is the gravitational acceleration, ε is eccentricity of the rotating parts, α is eccentricity margin for the flywheel (= 0.25), and N is the pump running speed.

The calculated results of the Radial Bearing loads are listed in Table 1. Because of the increased bearing span (L2 in Eqs.1 and 2), the radial thrust loads (Ra, Rb) on the bearings of the new RIP are smaller than the current RIP. The increase in the weight of the rotating parts and additional design margin for the eccentricity of the flywheel give larger unbalance loads (Fr). However, the increases in total radial loads are small and within the acceptable level.

Table 1 Radial Bearing load

	Current RIP	New RIP
Upper Bearing	100	104
Ra	84	72
Fr	16	32
Lower Bearing	62	68
Rb	46	36
Fr	16	32

Relative value when the Upper Bearing load of the current RIP equals 100 %.

2.4 Thrust Bearing Load

The Thrust Bearing load is affected by the increased weight of the rotating parts. Table 2 shows the calculated loads. The downward thrust load is increased by additional weights of the rotating parts. But this increase is evaluated within the development target.

Table 2 Thrust Bearing load

	Current RIP	New RIP
Upward	100	86
Downward	20	34

Relative value when the upward thrust load of the current RIP equals 100 %.

3. NEW RIP NOZZLE

3.1 Design of New RIP Nozzle

The RIP is supported by a nozzle of the RPV as shown in Fig.1. The nozzle has a sleeve-type configuration, and the air-gap between the RIP casing and the RPV has a function of securing symmetrical thermal expansion of the casing under operating conditions. The increased weight and length of the new RIP raise the seismic bending moment acted on the nozzle. In addition, a blanket load condition[2] that covers high seismic conditions of future ABWR sites is need to be considered in order to establish a standard nozzle design applicable to various site conditions. In order to withstand the enlarged design load, additional thickness is given to the nozzle as shown in Fig.2 and Table 3.

Table 3 Major dimensions of RIP Nozzle

	Current Nozzle	New Nozzle
Casing thickness*	35.5 mm	52.5 mm
Air-gap	18.0 mm	18.0 mm
Stub thickness*	48.5 mm	55.0 mm
Outside diameter	445.0 mm	492.0 mm

*Cladding thickness (4.0~7.5mm, depending on the location) is included.

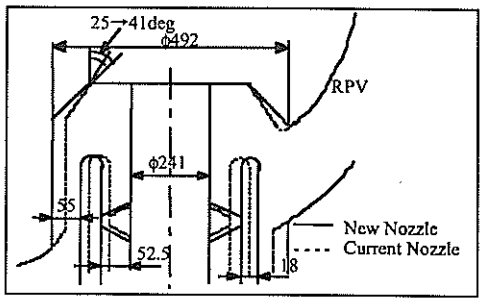

Fig.2 Schematic diagram of New Nozzle.

3.2 Stress Analysis

Two-dimensional FEM analyses were conducted to evaluate the strength of the nozzle using ABAQUS code. The computational grid used in the analyses is shown in Fig.3. The height of the nozzle stub is not symmetrical because the nozzle is located on the periphery of the RPV bottom head. The upper-side section that includes the shortest stub height was selected for the modeling because this model gives the most conservative result.

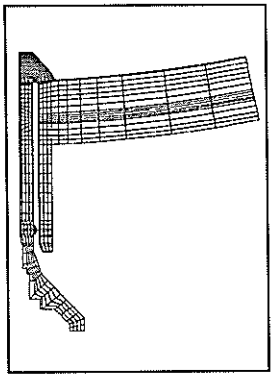

Fig. 3 Computational grid for stress analysis.

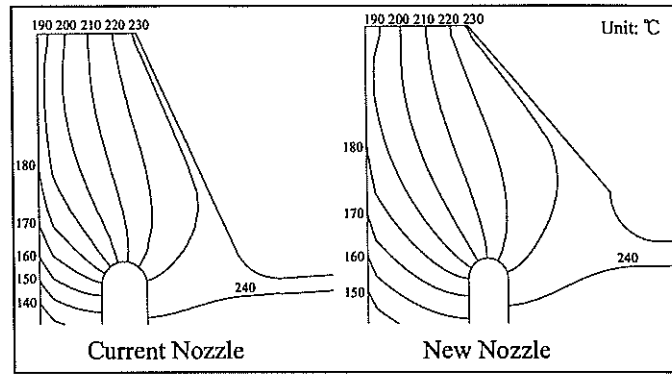

Fig. 4 Simulated temperature distribution in the generator trip event, one of the most rapid temperature- changing events.

Fig.4 shows predicted temperature distribution in the generator trip event, which is one of the most rapid temperature-changing events. Even though the thickness of the nozzle is increased, the temperature distribution is almost the same as those of the current design.

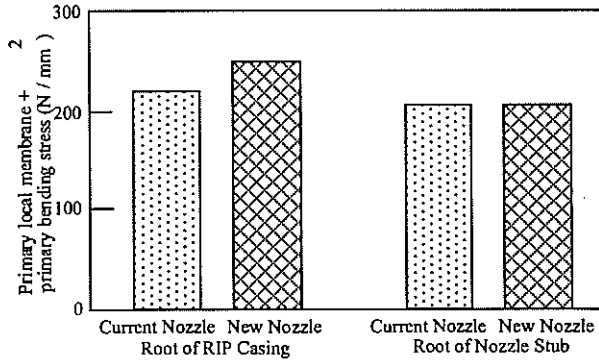

Fig. 5 Results of stress analysis for Design Condition.

Fig.5 shows the largest stress evaluated on the nozzle under the RPV design condition, i.e. Service Condition I, II (equivalent to Level A, B Service Limits) + S1 earthquake (maximum design earthquake). The largest stress (primary local membrane stress + primary bending stress) is estimated at the root of the casing. It is larger than the current design by 13 %, which is still within the design limit, even though the design moment load is 2.5 times larger than the current one.

3.3 Displacement Analysis

Three-dimensional FEM analyses were conducted using ABAQUS code to calculate the relative displacement between the Impeller and the Diffuser. The computational model used for the analyses is shown in Fig.6. The temperature distribution in the casing wall was calculated in the first step of the evaluation, and its good symmetrical nature was confirmed as shown in Fig.7. In the next step, the thermal and pressure deformations were calculated. The results listed in Table 4 reveal that the relative displacement between the Impeller and the Diffuser is slightly increased but within the design clearance.

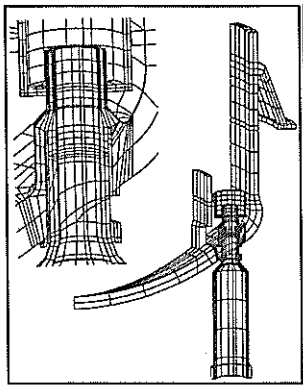

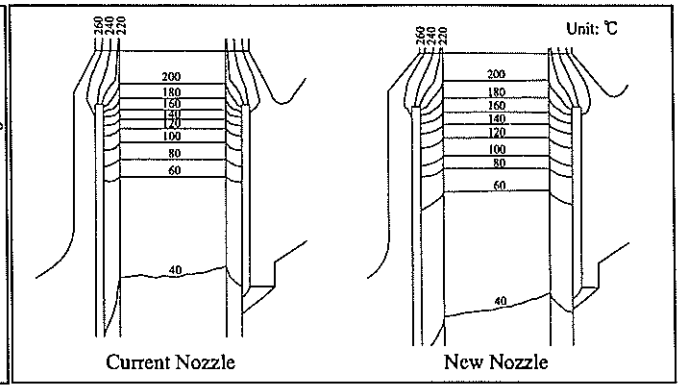

Fig.6 Computational model for displacement analysis.

Fig.7 Temperature distribution under normal operating condition.

Table 4 Calculated relative displacement between the Impeller and the Diffuser

	Relative displacement			Design gap
	Thermal displacement	Pressure displacement	Total	
New Nozzle	0.05 mm	0.09 mm	0.14 mm	1.0 mm
Current Nozzle	0.06 mm	0.06 mm	0.12 mm	1.0 mm

4. EFFECT OF ENLARGED NOZZLE ON PUMP DISCHARGE FLOW

4.1 Flow Analysis

The outside diameter of the new nozzle is increased from the current design because of the thicker casing and nozzle stab wall. In addition, its shoulder angle was changed in order to have the same nozzle height, i.e. the same overhang length of the Main Shaft from the upper Radial Bearing. The discharge flow of the RIP may be affected by those dimensional changes because the nozzle is located just downstream from the Diffuser.

Three-dimensional fluid analysis was conducted with STAR-CD code. The calculation conditions and the computational grid used in this analysis are shown in Table 5 and Fig.8 respectively.

Table 5 Calculation conditions

Item	Conditions
Turbulence model	$k-\varepsilon$ model
Scheme of advection term	First order upwind difference scheme
Inlet boundary	Uniform velocity
Outlet boundary	Zero gradient

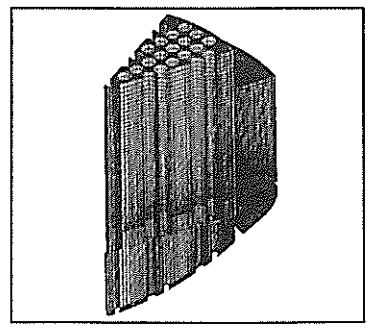

Fig.8 Computational grid for flow analysis.

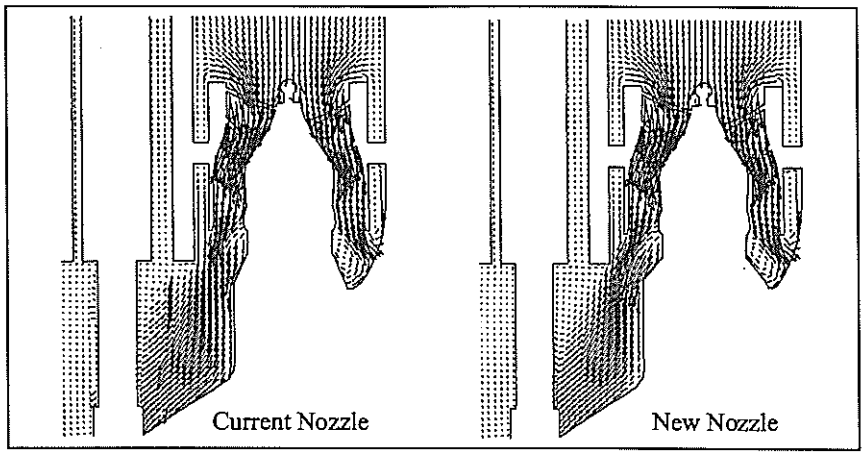

Fig. 9 Flow velocity distribution around Impeller, Diffuser and Nozzle.

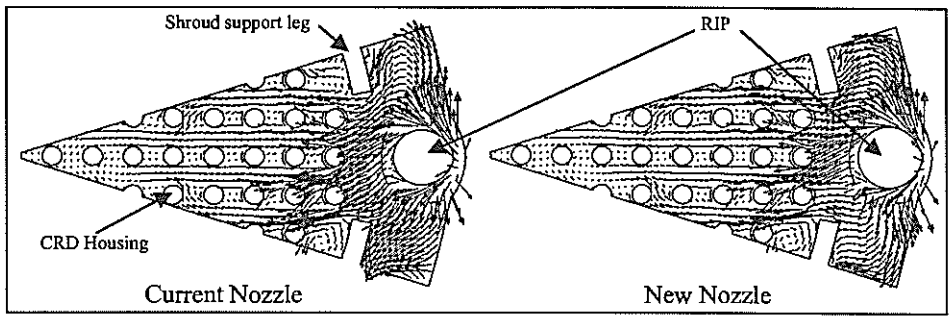

Fig. 10 Cross-sectional view of flow distribution in the RPV lower plenum.

The calculated velocity distributions are shown in Fig.9 and Fig.10. The difference between the velocity distributions of the current and new designs is evaluated to be very small. The pressure distribution was also evaluated, and it was estimated that an additional pressure loss of about 0.8 m is expected around the large new nozzle.

The radial thrust force acted on the Impeller is given by integrating the pressure distribution around the Impeller. The radial thrust force is evaluated to decrease with the increase of the nozzle diameter as shown in Fig.11. This is because larger nozzle has an effect of making more uniform pressure distribution around the nozzle, canceling the effect of the asymmetrical configuration of the discharge flow path.

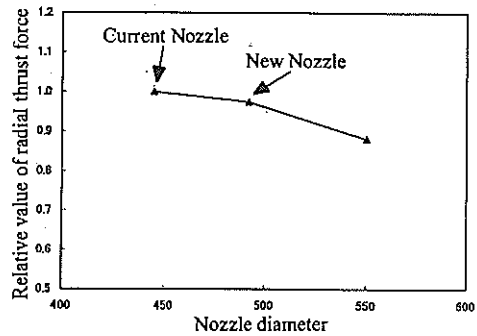

Fig. 11 Predicted radial thrust force.

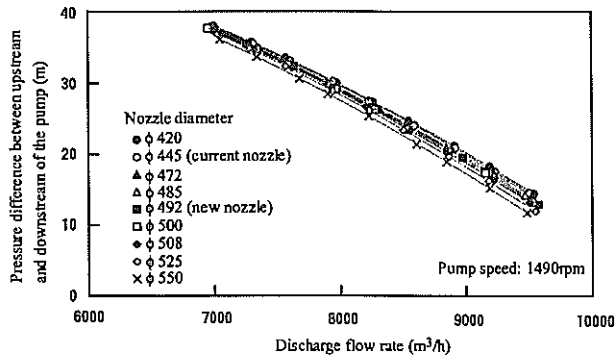

Fig. 12 Effect of the nozzle diameter on the pressure difference between upstream and downstream of the pump. (Calculated from 1/5-scale test data using the low of similarity.)

4.2 Model Flow Test

1/5-scale model flow tests were conducted with various diameters of the model nozzles at an elbow-loop test facility. The pressure loss grows bigger with increasing the nozzle diameter as shown in Fig.12. About 1 m of the pressure loss is expected for the new RIP nozzle form this result.

Following the 1/5-scale model tests, 1/1-scale tests were conducted at a test facility as shown in Fig.13. In this test, the model nozzle had a conservative diameter of 500 mm in order to confirm the effect of the enlargement of the nozzle. The pump speed in this test was 1340 rpm or smaller because of the limitation of the test facility, and the results were converted using the low of similarity in evaluating the performance under the rated condition.

The measured Q-H curve shown in Fig.14 exhibits a good characteristic of smooth inclination without any point of inflexion. The additional pressure loss due to the nozzle enlargement is evaluated to be about 1 m at the rated discharge flow rate based on this result. In order to compensate the additional loss, the required head of the new RIP is tentatively set at 41 m, increased by 1 m from the current specification. This tentative specification will be confirmed next year in the design confirmation tests of the new RIP and nozzle at a new full-scale test facility.

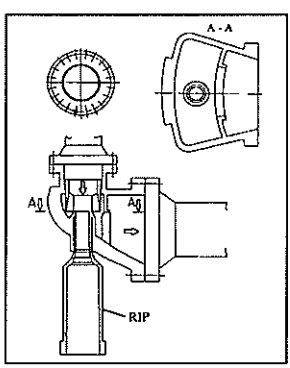

Fig.13 1/1-scale flow test facility.

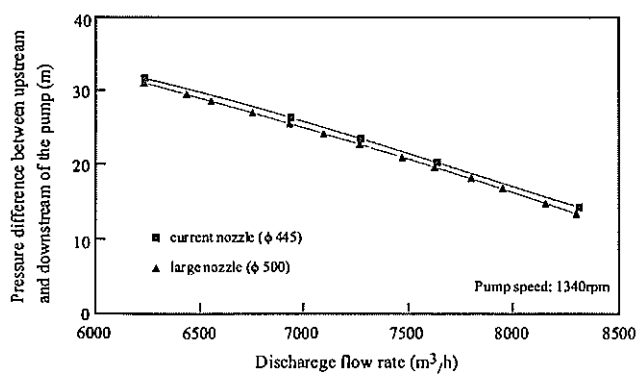

Fig.14 Measured pressure difference between upstream and downstream of the pump (1/1-scale test).

5. CONCLUSION

Basic Design of the simplified RIP system that eliminates the M-G sets in the power supply system was established. The newly developed RIP has a flywheel on the Main Shaft, and it is expected to have appropriate coast down characteristics without M-G sets. The new design of the RIP nozzle was also established according to the blanket design load condition that covers high seismic loads at various site locations. The effects of the enlarged RIP nozzle on the pump discharge flow were evaluated to be minimal. Based on these discussions, basic specifications of the new RIP system were established as listed in Table 6. This simplified RIP system will be the standard design for the Reactor Recirculation System of ABWR.

Table 6 Basic Specification of the Simplified RIP System

		Current RIP System	New RIP System
Pump:	Total head[1)]	40 m	41 m
	Discharge flow rate[1)]	2.14 m^3/s	2.14 m^3/s
	Moment of inertia	19.5 $kg*m^2$	45.0 $kg*m^2$
Power Supply:	M-G set	Two sets required	None
	Capacity	1250 kVA	1350 kVA
RIP Nozzle:	Diameter	445 mm	492 mm
	Sleeve thickness[2)]	35.5 mm	52.5 mm
	Stub thickness[2)]	48.5 mm	55.0 mm

1) A 111% core flow condition is considered.
2) Cladding thickness (4.0~7.5mm, depending on the location) is included.

REFERENCES

1. Endo, R., et al., "Further Improvement In ABWR (Part-2) Advanced Design Of RIP System," *Proc. of 7th International Conference on Nuclear Engineering*, Tokyo Japan, April 1999.
2. Okamura, Y., et al., "Development Of Inertia-Increased Reactor Internal Pump (RIP) And Large Size Nozzle," *Proc. of 7th International Conference on Nuclear Engineering*, Tokyo Japan, April 1999.